



Preparation of SiO₂ nanocomposites with aligned distributing glass fibre using freeze-drying process

Sen Liang^{1,*}, Xiao Zhang², Haibo Li¹, Min Luo¹, Mangmang Gao¹

¹Ningxia Key Laboratory of Photovoltaic Materials, Ningxia University, Yinchuan 750021, China

²School of Materials Science and Engineering, Beifang University of Nationalities, Yinchuan 750021, China

Received 16 November 2016; Received in revised form 16 May 2017; Received in revised form 11 August 2017;

Accepted 5 September 2017

Abstract

The glass fibre reinforced nano-SiO₂ composites (with up to 40 wt.% of glass fibres) as insulating materials were fabricated firstly by preparing aligned glass fibres under the ice formation followed by pressing and annealing. Scanning electron microscopy analyses confirmed the presence of parallel distribution of glass fibres in certain direction. The low-temperature nitrogen adsorption and mercury intrusion measurements showed that the composites have mesoporous structure with the mean pore size less than 20 nm. Further, it was found that the compressive strength and thermal conductivity of composite were 15.1 MPa and 0.0585 W/(m·K), respectively.

Keywords: silica based nanocomposites, glass fibre alignment, mesoporous materials, thermal properties

I. Introduction

Aerogels have been applied in many fields due to their unique structure [1]. Among aerogels, silica aerogel has attracted enormous attention owing to its high surface area and high porosity formed by nonmetal particles [2]. Since the pore sizes of silica aerogel are distributed from 2 to 50 nm, which is smaller than the mean free path of nitrogen and oxygen, the thermal conductivity caused by either the gas or the convection is very small [3]. However, the silica aerogel often suffers from poor mechanical performance that would restrict its application. Therefore, it is very important to improve the mechanical properties of silica aerogel by proposing and designing new approach [4]. Among various methods, fibres are often employed as reinforcement phase to strengthen the mechanical performance of the base material [1,5–12]. Wu *et al.* proposed a possible way to control the thermal and mechanical properties of fibre-reinforced aerogels composites by regulating the fibre alignments and the laminated structures [2,4]. Further, Takayuki *et al.* [13] synthesized porous ceramic material using a freeze-drying process, showing that the pores aligned along the macroscopic direction of ice for-

mation and acted as channels.

In this study, the glass fibre reinforced nano-SiO₂ aerogels as insulating materials were fabricated by preparing aligned glass fibres under the ice formation followed by pressing and annealing. Moreover, the effects of the fibre amount on the microstructure, heat insulation and the mechanical properties were analysed.

II. Experimental

2.1. Preparation

Nano-silica aerogel powders (QS20, Tokuyama Co., China), glass fibres (Zhongtian Junda Co., China) and polyvinyl alcohol (PVA, $M_w = 74800$ and 99% hydrolysed granule, the PVA quality fraction of PVA solution was 10%) were selected as raw materials. The mean particle size of silica aerogel powders was 25 nm. The length of fibre was 1–2 mm and the length-to-diameter ratio was greater than 100.

In a typical preparation, the total mass of nano-silica aerogel powders and glass fibres was 20 g; the weight percent of glass fibres was 10, 20, 30, and 40 wt.%. The silica aerogel powders, glass fibres, and PVA solution (56 ml) were added in deionized water (210 ml) under magnetic stirring for 2 h. Subsequently, it was dispersed ultrasonically for 1 h. After that, the obtained slurry was

*Corresponding author: tel: +86 0951 2062414, fax: +86 0951 2062414, e-mail: liangsen@nxu.edu.cn

poured into a cubic plastic container which was then immersed in a liquid nitrogen refrigerant. It should be noted that the liquid nitrogen should cover the bottom of the container. Meanwhile, the top of the container was opened so that the upper surface of the slurry was exposed to the atmosphere at room temperature. Thus, the ice was stimulated to grow parallel to the temperature gradient direction. After the slurry was completely frozen, the container was put into a drying vessel and dried for about 150 h under the temperature of 50 °C and vacuum of 10 Pa. The green compacts were carefully removed from the container, and then cut into appropriate size that suited for preparing samples with diameter of 20 mm and thicknesses of 3 and 20 mm, respectively. The compaction pressure was 50 MPa, and most of all, the loading force was perpendicular to the growth direction of ice. Finally, all samples were annealed at 800 °C. For comparison, samples with 10 and 20 wt.% of glass fibres were prepared by employing traditional powder metallurgy method. For convenience, the samples having glass fibres with aligned and random distribution are defined as GF-A and GF-R, respectively.

2.2. Characterization

The microstructures of the samples were investigated using a scanning electron microscope (VK-9700, KEYENCE Co., Japan). The pore size distributions were investigated by low-temperature nitrogen ad-

sorption (Nova2000e Quantachrome Co, U.S.A) and mercury porosimetry (AutoporeV, Micromeritics Co, U.S.A). The samples of $\varnothing 20 \text{ mm} \times 3 \text{ mm}$ were used to determine the thermal conductivity by steady-state heat flux method. In addition, the compressive strength was also measured (Instron 1195, Instron, USA).

III. Results and discussion

3.1. Microstructure of composite materials

Figures 1a and 1c show the SEM image of the GF-A composites containing 20 wt.% glass of fibres prepared by typical freeze-drying method after heat treatment at 800 °C. The inset in Fig. 1c is the same sample before the heat treatment. Obviously, glass fibres are distributed in parallel towards a certain direction. This resulted from the freeze-drying process where fibres were pushed by the ice during ice crystals growth from the bottom to the top surface of the gel. On the other hand, it was found that the glass fibres and SiO₂ nanoparticles linked together more tightly after heat treatment. Regarding formation of the GF-A composites, a possible mechanism was proposed by Zhang *et al.* [14] and the phenomenon could be explained by Mullins-Sekerka instability. Specifically, when target solution is frozen, ice crystals grow and solute species (glass fibres and SiO₂ nanoparticles) are excluded by these crystals. Because impurities have a very low solubility in ice crystals, a

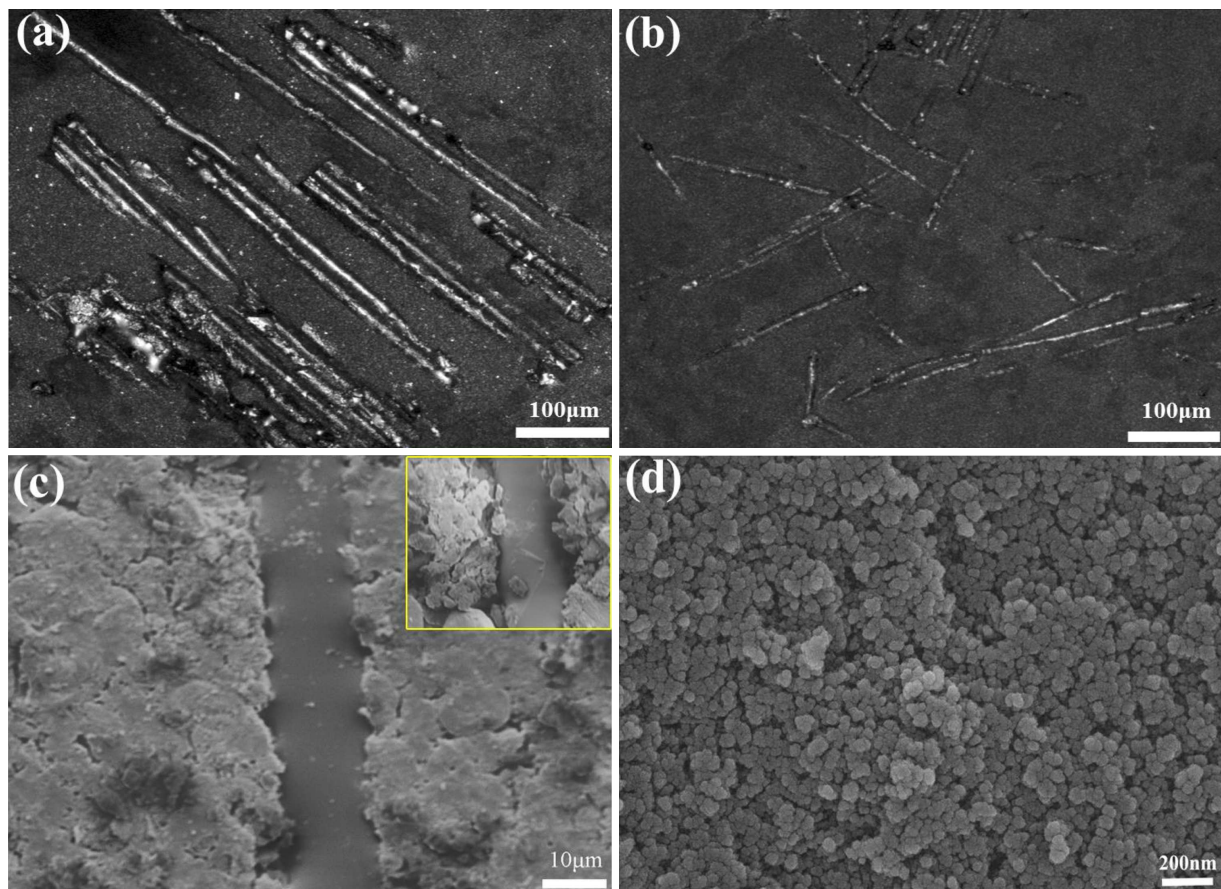


Figure 1. SEM micrographs of GF-A (a, c) and GF-R (b, d) containing 20 wt.% of glass fibres

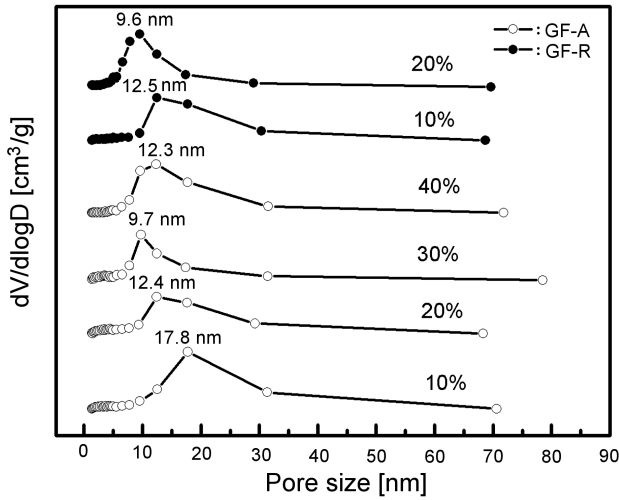


Figure 2. Pore size distribution determined by the N_2 adsorption-desorption

concentration gradient of the solute is formed and the solute concentration ahead of the ice front is increased. This increase in concentration reduces the melting point of the solution, which results in the formation of a constitutional supercooling zone and finally this can break down the planar interface, and the ice cell grows [14]. In our experiment, ice grows along the temperature gradient because the top of container was exposed to the air. Once the ice nucleated at the bottom of the container, the transition of heat from suspension to the cryogen would slow down and therefore the ice will grow in certain direction. Meanwhile, the ice crystals and glass fibres as well as SiO_2 nanoparticles were separated. Due to this, the glass fibres and SiO_2 nanoparticles are rearranged between the ice crystals. However, the distance between the ice crystals was far less than the length of the glass fibre, resulting in distribution of glass fibres in parallel to the direction of ice growth. Further, the ice would be sublimated via drying and thus the glass fibres could keep the certain arrangement. In addition, the SEM images of glass fibres with random distribution are shown in Figs. 1b and 1d. Clearly, fibres with a homogeneous porous nanostructure were cut off and

distributed in a random direction. Through comparison, it was suggested that the freeze-drying method should be a good choice to fabricate fibre aligned reinforced composite.

The porous texture of the composite, including pore volume and pore size, was investigated by Barrett-Joyner-Halenda (BJH) method. Both GF-A and GF-R composites have pore volume of 0.505–0.702 cm^3/g . Figure 2 shows the pore-size distribution determined by low-temperature nitrogen adsorption-desorption method. The mean pore sizes of the GF-A composites are 17.8, 12.4, 9.7 and 12.3 nm corresponding to composites having 10, 20, 30 and 40 wt.% of glass fibres. The GF-R composites with 10 and 20 wt.% of glass fibres have the mean pore sizes of 9.6 and 12.5 nm, respectively. Thus, both GF-A and GF-R are ascribed as mesoporous materials [15]. Likewise, the pore size distribution of the GF-R is similar with that of the GF-A composites, indicating that the pore size distribution of this composite is not dependent on the doping content of glass fibres as well as on the preparation. Furthermore, the mercury intrusion method was also employed to analyse the pore size of composites. It was showed that the mean pore size of as-prepared composite is less than 20 nm which is consistent with BJH analysis, indicating that the glass fibres reinforced silica aerogel composites are mesoporous materials.

3.2. Compressive strength and thermal conductivity

In the present study, glass fibres were used to enhance the mechanical properties of the silica aerogel. Figure 3a presents the compressive strength as a function of fibre content. When the glass fibres 10 to 30 wt.%, the compressive strength increased gradually. This showed that glass fibres are beneficial to improve the strength of the aerogel materials. Further, when the fibre loading content increased to a certain value, herein 30 wt.% of glass fibres, the strengthening effect reached a maximum. However, when the glass fibres exceeded 30 wt.%, fibres impeding-sintering effect became dominant and therefore the compressive strength of the composites decreased. In addition, Fig. 3a also shows that glass fibres

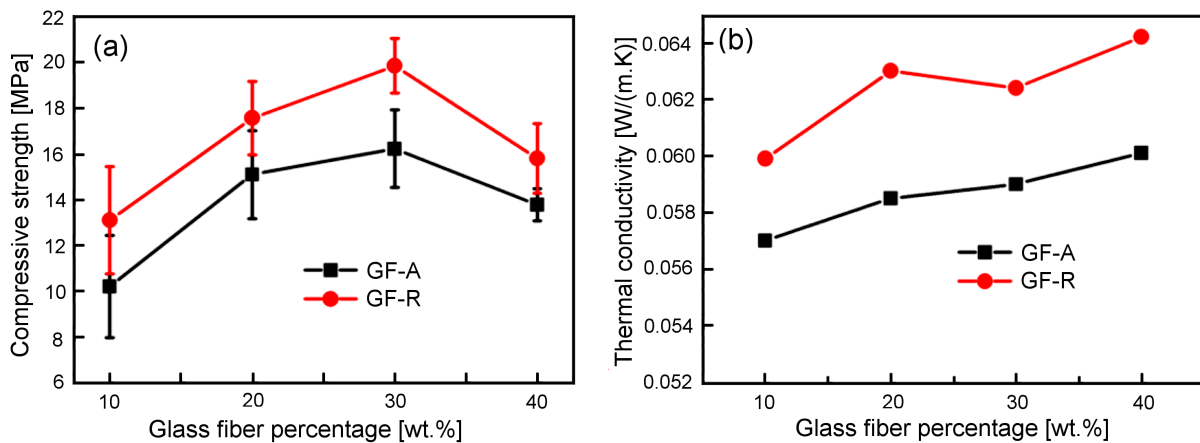


Figure 3. Compressive strength (a) and thermal conductivity (b) of GF-A and GF-R composites

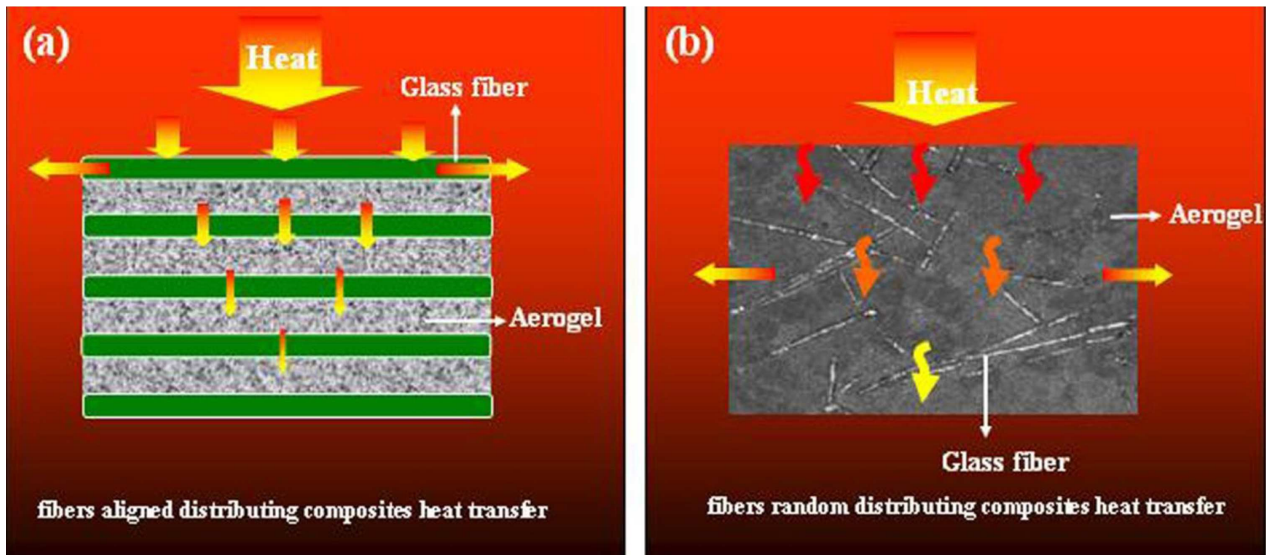


Figure 4. Schematic diagram of the heat transfer path in: a) GF-A and b) GF-R composites

reinforced composites prepared using different methods have similar function between compressive strength and the glass fibres content. Nevertheless, the compressive strength of the GF-A was lower than that of the GF-R composites at each certain glass fibre content, indicating that the strength of composite is associated with glass fibres' orientation.

Figure 3b shows the effect of the glass fibres addition on the thermal conductivity. The thermal conductivity of the GF-A composites increases from 0.057 to 0.0601 W/(m·K) with the increase of the glass fibres content from 10 to 40 wt.%. Yuan *et al.* [3] reported that silica aerogel/glass fibres composites fabricated by press forming method exhibit lower thermal conductivity (20 wt.% glass fibres, 0.025 W/(m·K) at 300 °C). This could be caused by the addition of TiO₂ as an opacifier. However, its' compressive strength was less than 1.2 MPa which was much lower than the present data, demonstrating that the heat treatment was favourable for improving the strength of the composites. It is known that the heat transfer can be achieved via three ways involving conduction, convection, and radiation. Basically, the heat transfer prefers conduction rather than radiation and conduction within the aerogel network is much smaller than in the pores. As a result, the radiation and heat transfer of the solids could be neglected. On the other hand, the mean pore sizes of the silica aerogel composites are less than 20 nm which is smaller than the mean free path of nitrogen and oxygen. In this case, the thermal conductivity contributed by the gas convection can be neglected. Figures 4a and 4b show the schematic diagram for heat transfer in the GF-A and GF-R composites, respectively. From Fig. 4a, it is observed that the aerogel is characterized by the aligned glass fibres. The filled aerogel restricted the heat transfer between glass fibres due to the low thermal conductivity of nano pores. However, from Fig. 4b, it could be obtained that the glass fibres are overlapped, leading to high heat transfer through the interconnected fibres.

IV. Conclusions

In this study, the glass fibre reinforced nano-SiO₂ composites as insulating material were fabricated by preparing aligned glass fibres under the ice formation followed by pressing and annealing. It was found that the obtained composites presented homogeneous mesoporous structure and the mean pore size was smaller than 20 nm. Further, the compressive strength of the composites increases with the increase of the glass fibres content from 10 to 30 wt.%. On the other hand, the thermal conductivity increases from 0.057, 0.0585, 0.059 to 0.0601 W/(m·K) with the increase of the glass fibres content from 10 to 40 wt.%, respectively. Besides, the thermal conductivity of the composite samples having glass fibres with aligned distribution is smaller than that of the samples with randomly distributed glass fibres due to the different heat transfer pathway.

Acknowledgements: This study was funded by the National Natural Science Foundation of China (No. 51302138, 21663001). Author Xiao Zhang appreciates the National Natural Science Foundation of Ningxia (No. NZ16085).

References

1. X. Yang, J. Wei, D. Shi, Y. Sun, S. Lv, J. Feng, Y. Jiang, "Comparative investigation of creep behavior of ceramic fiber-reinforced alumina and silica aerogel", *Mater. Sci. Eng. A*, **609** (2014) 125–130.
2. Y. Liao, H. Wu, Y. Ding, S. Yin, M. Wang, A. Cao, "Engineering thermal and mechanical properties of flexible fiber-reinforced aerogel composites", *J. Sol-Gel Sci. Techn.*, **63** [3] (2012) 445–456.
3. B. Yuan, S. Ding, D. Wang, G. Wang, H. Li, "Heat insulation properties of silica aerogel/glass fiber composites fabricated by press forming", *Mater. Lett.*, **75** [15] (2012) 204–206.
4. H. Wu, Y. Liao, Y. Ding, H. Wang, C. Peng, S. Yin, "Engineering thermal and mechanical properties of multilayer

- aligned fiber-reinforced aerogel composites”, *Heat Transf. Eng.*, **35** [11-12] (2014) 1061–1070.
5. Z. Jun-Jie, D. Yuan-Yuan, W. Xiao-Dong, W. Bu-Xuan, “An analytical model for combined radiative and conductive heat transfer in fiber-loaded silica aerogels”, *J. Non-Cryst. Solids*, **358** [10] (2012) 1303–1312.
 6. W.J. Lu, E.S. Steigerwalt, J.T. Moore, L.M. Sullivan, W.E. Collins, C.M. Lukehart, “Carbothermal transformation of a graphitic carbon nanofiber/silica aerogel composite to a SiC/silica nanocomposite”, *J. Nanosci. Nanotechnol.*, **4** [7] (2004) 803–808.
 7. J. Yang, S. Li, Y. Luo, L. Yan, F. Wang, “Compressive properties and fracture behavior of ceramic fiber-reinforced carbon aerogel under quasi-static and dynamic loading”, *Carbon*, **49** [5] (2011) 1542–1549.
 8. Y. Kong, X.-D. Shen, S. Cui, Y. Zhong, “Effect of carbothermal reduction temperature on microstructure of fiber reinforced silicon carbide porous monoliths with high thermal resistance”, *Chin. J. Inorg. Chem. Eng.*, **30** [12] (2014) 2825–2831.
 9. L. Xu, Y. Jiang, J. Feng, J. Feng, C. Yue, “Infrared-opacified Al₂O₃-SiO₂ aerogel composites reinforced by SiC-coated mullite fibers for thermal insulations”, *Ceram. Int.*, **41** [1] (2015) 437–442.
 10. Q.-F. Gao, J. Feng, C.-R. Zhang, J.-Z. Feng, W. Wu, Y.-G. Jiang, “Mechanical properties of aerogel-ceramic fiber composites”, *Adv. Mater. Res.*, **105-106** (2010) 94–99.
 11. Q. Gao, M. Feng, C. Zhang, J. Feng, W. Wu, Y. Jiang, “Mechanical properties of ceramic fiber-reinforced silica aerogel insulation composites”, *J. Chin. Ceram. Soc.*, **37** [1] (2009) 1–5.
 12. Z. Lu, Z. Yuan, Q. Liu, Z. Hu, F. Xie, M. Zhu, “Multi-scale simulation of the tensile properties of fiber-reinforced silica aerogel composites”, *Mater. Sci. Eng. A*, **625** (2015) 278–287.
 13. T. Fukasawa, M. Ando, T. Ohji, S. Kanzaki, “Synthesis of porous ceramics with complex pore structure by freeze-dry processing”, *J. Am. Ceram. Soc.*, **84** [1] (2001) 230–232.
 14. L. Qian, H. Zhang, “Controlled freezing and freeze drying: a versatile route for porous and micro/nano-structured materials”, *J. Chem. Technol. Biot.*, **86** (2011) 172–184.
 15. C.Y. Kim, J.K. Lee, B.I. Kim, “Synthesis and pore analysis of aerogel-glass fiber composites by ambient drying method”, *Colloids Surf. A*, **313** (2008) 179–182.